



Performance and thermal charging/discharging features of a phase change material assisted heat pump system in heating mode



Fuxin Niu^a, Long Ni^b, Yang Yao^b, Yuebin Yu^{a,*}, Haorong Li^a

^aDurham School of Architectural Engineering and Construction College of Engineering, University of Nebraska-Lincoln, Omaha, USA

^bSchool of Municipal and Environmental Engineering, Harbin Institute of Technology, Harbin, China

HIGHLIGHTS

- We introduced an integrated heat pump with a triple-sleeve energy exchanger.
- Experiments were carried out to investigate the performance and thermal behavior.
- Dynamic balance was observed between water and refrigerant with a PCM interlayer.
- The system with a PCM interlayer had a high COP value.

ARTICLE INFO

Article history:

Received 22 January 2013

Accepted 25 April 2013

Available online 13 May 2013

Keywords:

Phase change material

Heat pump

Thermal storage

Dynamic balance

ABSTRACT

At low ambient temperature, air-source heat pump suffers from decrease in both heating capacity and coefficient of performance (COP), and increase in compressor's pressure ratio. A parallel triple-sleeve energy storage exchanger with phase change material (PCM) for storing thermal heat was designed to ensure the reliable operation of a heat pump under various weather conditions and enhance the system performance at low ambient temperature. The innovative device also includes a solar thermal collector loop for utilizing free solar energy. Thermal heat can be transferred into and stored by the PCM using water as the heat transfer medium. Controlled experiments were carried out to investigate the performance and the simultaneous thermal charging and discharging behavior of this enhanced heat pump system. Transient operating characteristics, including the temperatures, pressures and heat transfer rate, were analyzed. The COP value in an operating mode with a constant heat transfer fluid water temperature and flow rate increased until the system entered into the stable operating stage. The final COP can reach up to 3.9 when the three heat transfer mediums (water/PCM/refrigerant) achieved the steady-state. The experimental results show an interesting phenomenon that the heat transfer process between water and refrigerant with a PCM interlayer was a dynamic balance. The PCM temperature and the difference of the water temperature at the inlet and outlet of the evaporator regularly fluctuated around some balance points. In this study, the measured PCM temperatures in the dynamic steady-state were 12.8 and 14.2 °C. The difference of the water temperature at the inlet and outlet of the evaporator balanced around 2.8 °C. The findings in the research implied more study is needed to explore the PCM charging/discharging mechanisms and improve the operation of the PCM assisted thermal system.

© 2013 Elsevier Ltd. All rights reserved.

1. Introduction

With the rapid development of economy and the increasing energy demand, energy conservation draws more and more public

attention. Compared to those traditional gas or electric water heater, air-source heat pump (ASHP) can serve the same purpose with two- to three-time higher efficiency [1,2]. Therefore, ASHP is gradually used in residential and commercial buildings for heating applications, providing significant economic benefits. In southern China, especially in the Yangtze River delta, extreme low surrounding temperature can reach -10 °C in winter. Supposing the set point of outlet water temperature is 55 °C, the working temperature range of ASHP would reach to 65 °C. At low ambient temperatures, the heating capacity of ASHP drops rapidly. The high pressure ratio on the refrigerant side is likely to cause high/low

* Corresponding author. University of Nebraska-Lincoln, Durham School of Architectural Engineering and Construction College of Engineering, Room PKI 104F, 1110 S67th St, Omaha 68182, United States. Tel.: +1 402 554 2082; fax: +1 402 554 2080.

E-mail addresses: yuebinyu@gmail.com, yuebin.yu@unl.edu (Y. Yu).

Nomenclature

ASHP	air-source heat pump
COP	coefficient of performance
HTF	heat transfer fluid
PCM	phase change material
TRESE	triple-sleeve energy storage exchanger

pressure protection and trip off the system. In addition, the low operating temperature of the outside air heat exchanger can cause frosting on the surface and lead to decrease in the performance. Therefore, some assisted devices and technologies such as auxiliary heaters have been researched and applied to the ASHP for improving the performance under the low temperatures [3–5].

In recent years, thermal energy storage is playing an increasing important role in energy conservation applications. Since PCM has high heat storage density and a narrow range of operating temperature during a phase change, it is widely used in thermal systems for storing thermal energy [6]. Many experiments have been conducted to study the thermal performance of PCM storage system [7–9]. According to these publications, paraffin waxes can be found in many applications and is the most widely used one. However, its inherent disadvantage of low heat transfer rate during the charging/discharging process limited the improvement of thermal performance. For various circumstances, composite materials consisting of a PCM and at least one other material might be applied instead. The other material serves to improve one or more the PCM properties (e.g. melting temperature, specific heat, etc.). For example, the use of graphite particles and fibers PCM has been proposed about ten years ago to enhance the thermal conductivity [10]. Since then, numerous publications have experimentally proved this concept with different composite PCM. A new supported phase change material made of paraffin impregnated by capillary forces in a compressed expanded natural graphite matrix was presented by Py [11]. Composite PCM/CENG thermal conductivities were found to be equivalent to those of the sole graphite matrix from 4 to 70 W/(m K), much higher than 0.24 W/(m K) of the pure paraffin. Zhang and Fang [12] experimentally studied the thermal performance of a paraffin/expanded graphite composite phase change material. The heat transfer rate of the paraffin/expanded graphite composite was observed higher than that of the paraffin due to the high thermal conductivity of the combined expanded graphite. The prepared paraffin/expanded graphite composite PCM had a large thermal storage capacity and did not experience liquid leakage during its solid–liquid phase change. Medrano et al. [13] experimentally investigated the heat transfer process during melting (charge) and solidification (discharge) of five small scale heat exchangers working as latent heat thermal storage systems. Results showed that the double pipe heat exchanger with the PCM embedded in a graphite matrix is the one with higher values, ranging from 700 to 800 W/(m² K). It could be concluded that increase of the heat transfer coefficient was more important than increase of heat transfer area. Sole et al. [14] conducted several charging tests to investigate the performance of a hot water tank with about 90 vol.% of sodium acetate trihydrate and 10 vol.% graphite as PCM. Energetic and exegetic analyses were conducted for the charging of the water tank, with and without PCM, to clarify the contribution of PCM. Since the 1950s, many researchers have studied various solar assisted heat pumps [15–18]. Han et al. [19] built up a mathematical model for a solar assisted ground-source heat pump with an energy storage device, and studied the effect of the heat storage device on the performance of the solar assisted ground-source heat pump. Ozgener and

Hepbasli set up a greenhouse heating system based on a solar assisted ground-source heat pump and studied its operating characteristics [20]. The effect of pipe work arrangement on the performance of the solar assisted ground-source heat pump heating system was also investigated. A direct-expansion solar assisted heat pump system, which could offer space heating in winter and air conditioning in summer and supply hot water throughout a year, was also studied [21]. Xu et al. [22] proposed a new type of solar-air source heat pump water heater, whose flat-plate heat collector/evaporator with spiral-finned tubes could extract energy from both solar irradiation and ambient air for hot water heating. The operating performances of the system were simulated. Li et al. [23] built up a direct-expansion solar assisted heat pump water heater, studied experimentally the system performance and finally proposed some measures for system optimization.

It is a new idea to combine an ASHP with thermal storage technology and solar collecting system. The integrated system utilizes the PCM for heat storage and improves the performance of the heat pump at low ambient temperatures. In addition, a solar energy system is included to collect solar energy for thermal storage and directly space heating. Based on the idea, the authors designed a novel integrated heat pump system with triple-sleeve energy storage exchanger (TRESE) [24]. This novel compact heat pump system cannot only make use of off-peak electricity to provide low-cost space heating/cooling and hot water, but also ensure the reliable operation under various weather conditions. In our previous work, experiments on thermal performance of triple-sleeve energy storage exchanger have been carried out to verify the feasibility of the integrated heat pump system. In this paper, we presented and discussed the transient operating characteristics, including the temperatures, pressures and heat transfer rate, of the system.

In the following sections, we first briefly introduced the structure of the integrated heat pump system. Then we described the settings and the testing procedure of the experiments. The results of the trended data and the derived variables are then presented to interpret the performance of the system. The paper finally concluded with a brief discussion on the observed phenomenon.

2. Integrated heat pump system (with triple-sleeve energy storage exchanger)

2.1. The structure of TRESE

A new integrated heat pump system with TRESE has been proposed. Its key component TRESE had a special structure. Fig. 1 shows the detailed structure of an energy storage cell used in the TRESE. It consisted of three passes of concentric copper tubes. PCM was embedded inside the space between the outer tube and the inner tube. Refrigerant flowed inside the inner tube and heat

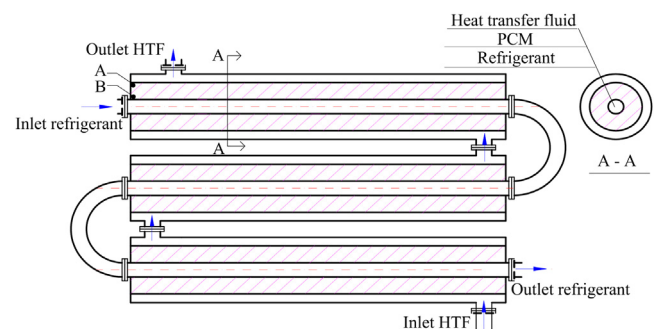


Fig. 1. Structure of an energy storage cell used in the TRESE [24].

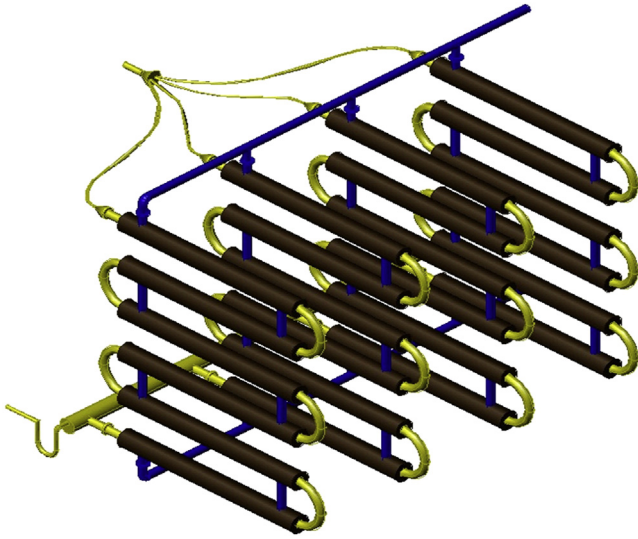


Fig. 2. Three-dimensional picture of the TRESE.

transfer fluid water flowed in the outer tube. Fig. 2 shows three-dimensionally a TRESE with four energy storage cells. In the integrated system, the TRESE not only was operated as the device storing solar energy for solving intermittence and instability of solar energy, but also acted as an evaporator of a heat pump. At low ambient temperatures, a conventional ASHP suffers from decrease in both heating capacity and coefficient of performance. Therefore, the refrigerant flow was tuned from outside air heat exchanger to TRESE so as to increase the evaporation temperature and improve the performance of heat pump.

2.2. The selection of PCM

The triple-sleeve energy storage exchanger is a cooling storage device in summer and is also a heat storage device in winter. In order to meet the demands of both heat and cooling storage, appropriate PCM must be selected. Therefore, a PCM whose phase change temperature is 6 °C was embedded in TRESE. In summer, with the supply and return temperatures of the HTF being 7 °C and 12 °C, respectively, cooling energy generated and stored in PCM could be used for space cooling via HTF. In winter, the HTF temperature was designated at 20 °C for improving the efficiency of solar collectors, and heat energy from the HTF can be stored in PCM. In addition, latent heat of PCM should be sufficiently large to avoid a bulky TRESE. Table 1 shows the thermal properties for the selected PCM.

2.3. The structure of integrated system with TRESE

The schematic diagram of the integrated system is shown in Fig. 3. It combined solar thermal and air source heat pump coupled

Table 1
Characteristic parameters of RT6.

Characteristic	Unit	Value
Phase change temperature	°C	6
Latent heat	kJ/kg	183
Density (solid/liquid)	kg/m ³	860/750
Volume expansibility	%	10
Specific heat (solid/liquid)	kJ/kg K	1.8/2.4
Thermal conductivity	W/(m K)	0.4

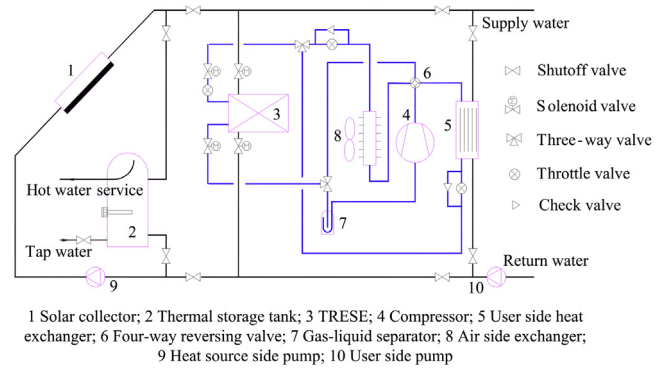


Fig. 3. Schematic diagram of the integrated heat pump system with triple-sleeve energy storage exchanger.

through a key component TRESE. The system can realize multi-functions by regulating the valves to simultaneously relieve the problems of inefficiency, instability and frosting at the lower temperature conditions in winter. In summer, cooling energy could be

Table 2
Operating modes and their operating conditions.

Operating mode name	Operating conditions
Mode 1 Solar heat pump heating mode in winter	When outdoor air temperature is low and solar energy is available, e.g., at daytime, and the energy stored in PCM is adequate to meet the space heating demand, the heat pump takes energy from the PCM for space heating.
Mode 2 Heat storage mode in winter	The mode is applied in transition season in winter when sunlight is abundant, but without heating demand. Solar energy is stored in PCM of the TRESE using HTF.
Mode 3 Direct heating using solar energy in winter	When sunlight is abundant and solar energy available exceeds heating demand, solar energy can be used for space heating.
Mode 4 Heat pump based heating using energy stored in PCM in winter	When outdoor air temperature is low or solar energy is not available, e.g., at night, and the energy stored in PCM is adequate to meet the space heating demand, the heat pump takes energy from the PCM for space heating.
Mode 5 Air source heat pump based heating in winter	When there is no solar energy supply, the air source heat pump can be operated for space heating in winter.
Mode 6 Air source heat pump based cooling and solar hot water supply in summer	When hot water supply is needed, but there is no need to store cold energy in PCM, the air source heat pump and the solar collectors are operated for space cooling and hot water supply, respectively.
Mode 7 PCM cold storage at night in summer	When there is no space cooling demand at night, cold energy generated by using the air source heat pump at the valley price of electricity is stored in the PCM.
Mode 8 PCM cold discharge at daytime in summer	At daytime when electricity price is high, cold energy generated and stored in PCM at nighttime is released for space cooling.
Mode 9 Air source heat pump cooling and cold discharge in summer	When the cold energy stored in PCM cannot meet the cooling demand at daytime, both the air source heat pump and the cold energy stored in PCM at night are used for space cooling.

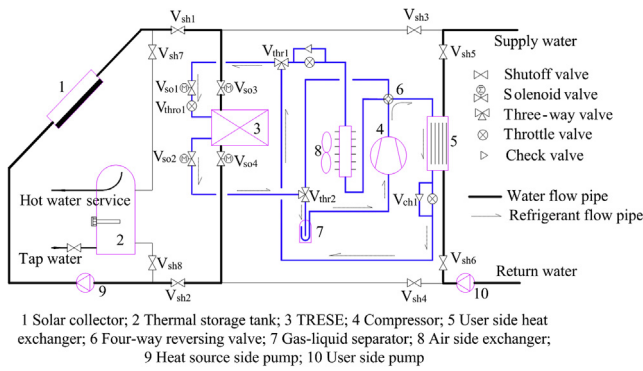


Fig. 4. Flow chart of experimental system.

accumulated in PCM of TRESE by an ASHP in cooling mode at valley electricity price in the nighttime. In the daytime, cooling energy was released through heat transfer between water and PCM at peak electricity price. It achieved the objectives of reducing peak and filling valley for easing the pressure on electricity and saving the operating cost. Meanwhile, the efficiency of air source heat pump increased due to the lower air temperature in the nighttime. In winter, the water carrying heat energy from the solar collectors flowed into the TRESE and charged the energy into PCM. When the ambient air temperature was low, the TRESE acted as the evaporator of heat pump for space heating. The integrated system combined cold storage in summer and heat storage in winter makes extensive use of advantages of heat pump technology and energy storage technology.

With the opening/closing of the solenoid valves and shutoff valves, the following nine different operating modes can be realized. Table 2 shows these nine operating modes and their operating conditions.

The optimal operation of the integrated system can automatically switch among the nine operating modes to adapt to various weather conditions all year round. With such a system, the utilization of solar energy, energy efficient heat pump technology, PCM based thermal energy storage technology, can be realized.

3. Experimental system and procedure

The integrated system reported in Section 2 has nine different operating modes; therefore it can be used continuously on a yearly base at different weather conditions. Mode 1: solar heat pump heating mode in winter was special one among all operating modes. It contained simultaneous thermal charging and discharging behavior based on PCM. An experimental study has been carried out and reported in the following sections.

A test rig was established to investigate the transient operating characteristics of the integrated system. Fig. 4 shows the flow chart of experimental system. Thick black and solid lines stand for the water flow directions and the dotted lines with arrows stand for the refrigerant flow directions. In order to realize the mode the valves were controlled by open or close. Table 3 shows the valves positions in the mode 1 condition.

Table 3
Valves positions in mode 1 condition.

Positions	Valves
Open	V _{sh1} , V _{sh2} , V _{sh5} , V _{sh6} , V _{so1} , V _{so2} , V _{so3} , V _{so4}
Close	V _{sh3} , V _{sh4} , V _{sh7} , V _{sh8} ,

Table 4
Configuration of the TRESE used in the experimental setup.

Characteristic	Value	Unit
Inner pipe diameter	8	mm
Middle pipe diameter	28	mm
Outer pipe diameter	40	mm
Energy storage volume	11,500	ml
Pipe length	24	m
Number of storage cell	4	–

The specification of the TRESE used in the setup is collected in Table 4. A rotary compressor with a rated cooling capacity of 980 W was used, and R22 was selected as the refrigerant. Two water tank with temperature and flow controlled were used to simulate solar and user side water conditions. The heat sink on the condenser side of the heat pump was emulated with a constant water flow at rate 0.055 kg/s and temperature at 40 °C. 20 °C hot water at a constant mass flow rate 0.044 kg/s was fed into the outer tube of the TRESE. It coupled with the PCM and the evaporator of the heat pump. The main measurements that have been recorded are: water flow rate, water temperature, PCM temperature, refrigerant temperature, and refrigerant pressure. The setup included a data acquisition system of high accuracy. The water flow rate was measured by rotary flow meter (of ±2% accuracy). Water temperatures at both the inlet and outlet of the TRESE and condenser were measured by T-type thermocouples (of ±0.3 °C accuracy). Two T-type thermocouples were located in points A and B (as shown on Fig. 1) to measure the PCM temperature. Compressor suction and exhaust pressures were measured by pressure sensors (of ±0.25% accuracy). The experimental data were regularly recorded with a time interval of 1 s.

4. Experimental results

Fig. 5 plots the trended compressor suction and exhaust pressure. The results indicated that the system entered the steady operation quickly after about 100 s starting period. During the stable operation, exhaust pressure kept at a constant value of 1.98 MPa and suction pressure remained at 0.6 MPa. During the whole process, except for unstable operating stage at the beginning, the average compression ratio was about 3.3. Fig. 6 illustrates the refrigerant temperature at the inlet and outlet of TRESE. The refrigerant temperature at the inlet and outlet of TRESE declined quickly at the beginning. And the rate of change at the inlet refrigerant temperature is larger than that of the outlet. The refrigerant temperature at

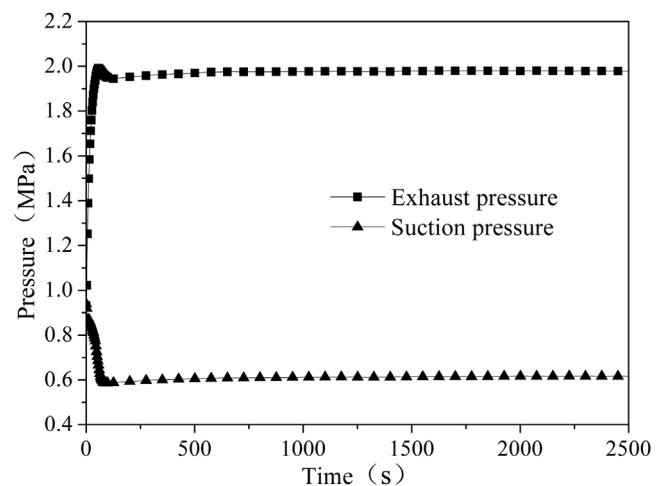


Fig. 5. Compressor suction and exhaust pressure.

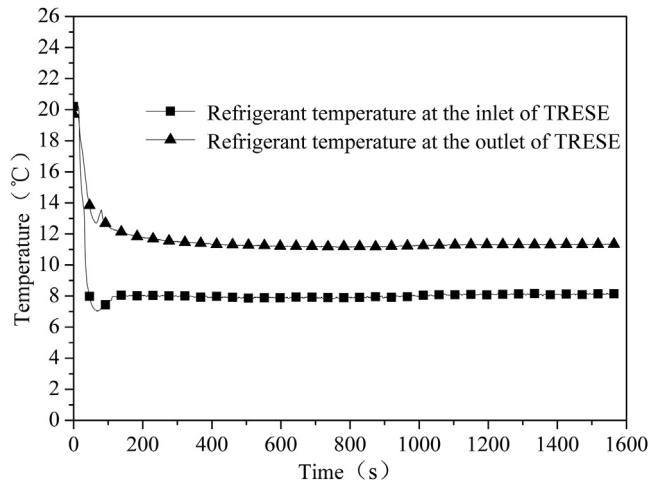


Fig. 6. Refrigerant temperature at the inlet and outlet of TRESE.

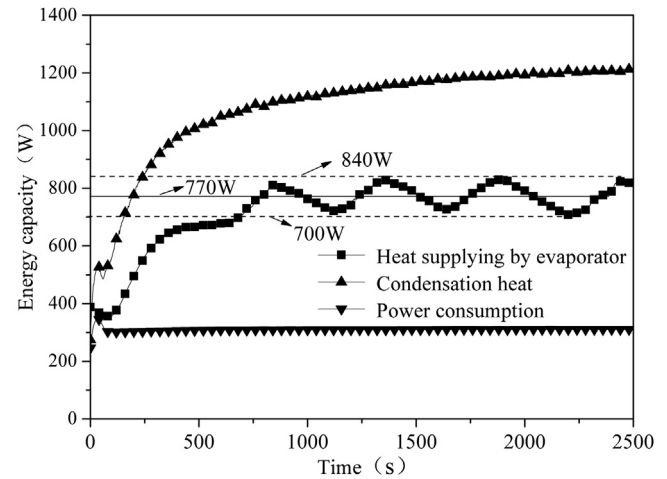


Fig. 8. Energy capacities of the PCM assisted heat pump in heating mode.

inlet of TRESE kept at a value of 8 °C in the stable operating stage. The refrigerant temperature at the outlet of TRESE kept at a value of 11.5 °C. Therefore, the experimental results illustrated that the degree of superheat of the heat pump was 3.5 °C.

Fig. 7 shows the temperature difference of the heat transfer fluid water at the inlet and outlet of both the evaporator and condenser. As can be seen from the figure, the temperature difference rose rapidly in the first 400 s. After that the rising rate of the temperature difference at the inlet and outlet of the condenser slowed down. It finally settled at 4 °C. For the evaporator side, it took about 700 s for the temperature difference of the thermal water at the inlet and outlet of the evaporator to enter a dynamic balance. The temperature difference fluctuated around the balance point of 2.8 °C and remained in a range of 2.45 °C–3.2 °C. Based on the temperature differences of the heat transfer water and the associated mass flow rates, the energy analysis can be obtained. Fig. 8 shows the energy capacities of simultaneous thermal charging and discharging of the integrated heat pump system. As can be seen from the figure, the condensation heat increased quickly in the first 700 s. After that, the rising rate slowed down and at last the condensation heat kept at a value of 1200 W. Power consumption of the heat pump was stable at 310 W.

The plot shows that the heat supplied by the evaporator included two stages: rising stage and dynamic balance stage.

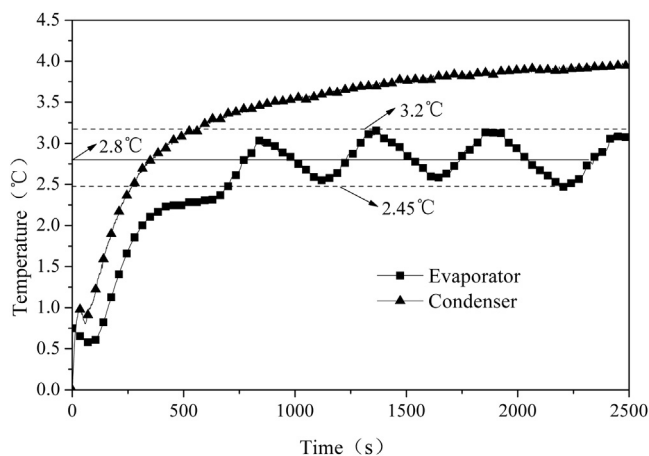


Fig. 7. Water temperature difference between the inlet and outlet of both evaporator and condenser.

During the first stage, heat absorbed by the evaporator increased rapidly to 680 W in the beginning of 700 s. Since then, the amount of heat fluctuated between 700 W and 840 W, centered at 770 W. Fig. 9 shows the COP of the PCM assisted heat pump. The COP rose rapidly to 3.3 in 500 s and reached slowly to 3.9 in the end.

In order to obtain the characteristics of the PCM, two measurement points A and B (a distal and proximal at the inlet of the evaporator as shown in Fig. 1) were set up. Fig. 10 plots the temperatures of PCM at the two locations. As shown in this figure, the PCM temperatures contained two stages: rapidly decline stage and dynamic balance stage. The PCM temperature at point A fluctuated around the balance point of 14.2 °C at dynamic balance stage. The PCM temperature at point B fluctuated around the balance point of 12.8 °C. The difference in the PCM temperatures at points A and B kept at 1.4 °C.

The experimental results shown above indicated that the PCM thermal charging/discharging of the system during the stable operating stage was a dynamic process. It appeared that the charging and discharging of the PCM was happening alternatively and at different rates. The phenomenon was further investigated through the comparison between the energy change of PCM and the heat absorbed by the evaporator, shown in Fig. 11. Based on energy conservation, the energy change of PCM is equal to the difference of the sum of heat pump power consumption and heat absorbed/supplied by the evaporator and the condenser. Positive or

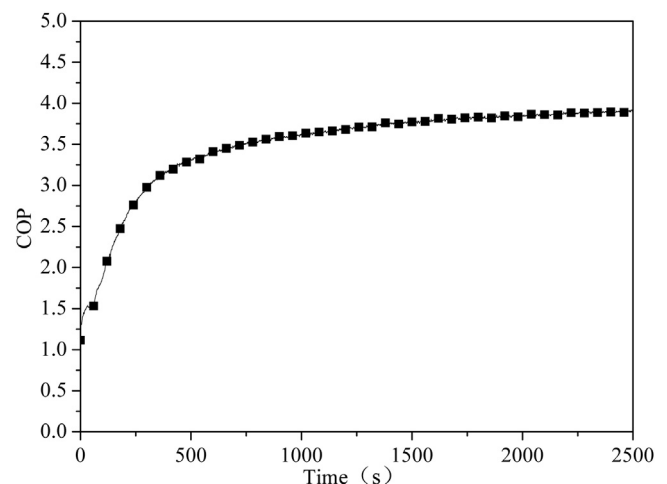


Fig. 9. COP of the heat pump in the controlled experiment.

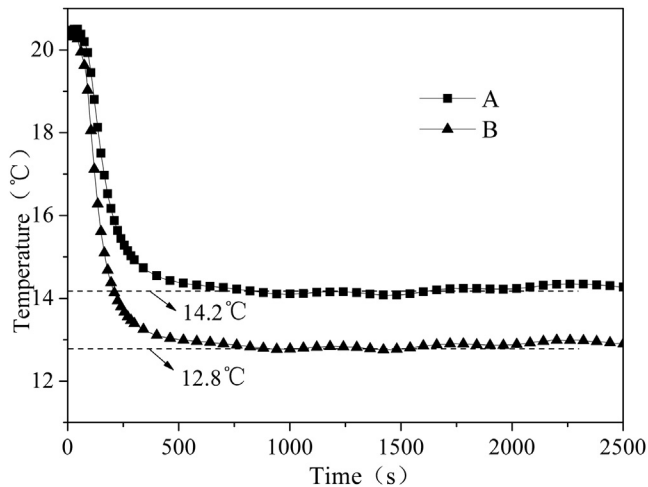


Fig. 10. PCM temperatures at Point A and B.

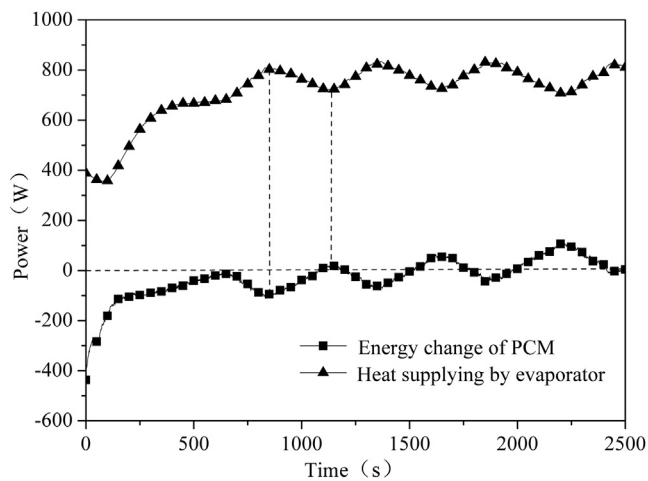


Fig. 11. Comparison of energy change in PCM and heat absorbed by the evaporator.

negative values stood for the two directions of accumulating and discharging energy respectively. The negative energy change of PCM in the beginning of 1100 s indicated that the energy stored in the PCM was discharged to the evaporator. After that, the positive and negative values came out alternately, which means that the processes of energy accumulated and discharged happened alternately. As can be seen from the figure, when the energy change of PCM was at the valley, the heat absorbed by the evaporator was at the peak. The two processes fluctuated synchronously.

5. Conclusions

Air source heat pump system with a parallel triple-sleeve energy storage exchanger with PCM was designed to ensure the reliable operation under various weather conditions and enhance the system performance at low ambient temperature. In this paper the performance and thermal charging/discharging features of the PCM assisted heat pump system in heating mode were studied. The COP of the heat pump system with a PCM interlayer rose quickly and could reach up to 3.9 at last. The controlled experiments also showed that the PCM acted as a heat transfer buffering medium between the refrigerant and water. The heat transfer process between water and refrigerant with a PCM interlayer was found as a dynamic balance process. The PCM temperature and the difference

of the water temperature at the inlet and outlet of the evaporator regularly fluctuated around some balance points. In this study, the measured PCM temperatures in the dynamic steady-state were 12.8 and 14.2 °C. The difference in the water temperature at the inlet and outlet of the evaporator fluctuated around 2.8 °C, from 2.45 to 3.2 °C. It appeared that the charging and discharging of the PCM was happening alternatively and at different rates. The findings in the research implied more study is needed to explore the PCM charging/discharging mechanisms and improve the operation of the PCM assisted thermal system.

Acknowledgements

The authors wish to acknowledge the funding supports from National Natural Science Foundation of China (Grant No. 51178133) and Industry-Academia-Research project combined Guangdong Province with Ministry of Education (Grant No. 2011B090400148).

References

- [1] P. Neksa, H. Rekestad, G.R. Zakeri, P.A. Schiefloe, CO₂-heat pump water heater: characteristic, system design and experimental results, *Int. J. Refrig.* 21 (1998) 172–179.
- [2] J. Ji, T.T. Chow, G. Pei, J. Dong, W. He, Domestic air-conditioner and integrated water heater for subtropical climate, *Appl. Therm. Eng.* 5 (2003) 581–592.
- [3] D. Liu, F.Y. Zhao, G.F. Tang, Frosting of heat pump with heat recovery facility, *Renew. Energy* 32 (2007) 1228–1242.
- [4] Y. Yao, Y.Q. Jiang, S.M. Deng, Z.L. Ma, A study on the performance of the airside heat exchanger under frosting in an air source heat pump water heater/chiller unit, *Int. J. Heat Mass Transfer* 47 (2004) 3745–3756.
- [5] Z.Y. Wang, X.M. Wang, Z.M. Dong, Defrost improvement by heat pump refrigerant charge compensating, *Appl. Energy* 85 (2008) 1050–1059.
- [6] E.S. Fath Hassan, Heat exchanger performance for latent heat thermal energy storage system, *Energy Convers. Manage.* 31 (1991) 149–155.
- [7] I.M. Bugaje, Enhancing the thermal response of latent heat storage systems, *Int. J. Energy Res.* 21 (1997) 759–766.
- [8] D. Pal, Y. Joshi, Application of phase change materials for passive thermal control of plastic quad flat packages: a computational study, *Numer. Heat Transfer* 30 (1996) 19–34.
- [9] D.W. Hawes, D. Feldman, D. Banu, Latent heat storage in building materials, *Energy Buildings* 20 (1993) 77–86.
- [10] J. Banaszek, R. Domanski, M. Rebow, Numerical analysis of the paraffin wax–air spiral thermal energy storage unit, *Appl. Therm. Eng.* 4 (2000) 323–354.
- [11] X. Py, R. Olives, S. Mauran, Paraffin/porous-graphite-matrix composite as a high and constant power thermal storage material, *Int. J. Heat Mass Transfer* 14 (2001) 2727–2737.
- [12] Z.G. Zhang, X.M. Fang, Study on paraffin/expanded graphite composite phase change thermal energy storage material, *Energy Convers. Manage.* 3 (2006) 303–310.
- [13] M. Medrano, M.O. Yilmaz, M. Nogues, J. Roca, L.F. Cabeza, Experimental evaluation of commercial heat exchangers for use as PCM thermal storage systems, *Appl. Energy* 10 (2009) 2047–2055.
- [14] C. Sole, M. Medrano, A. Castell, M. Nogues, H. Mehling, L.F. Cabeza, Energetic and exergetic analysis of a domestic water tank with phase change material, *Int. J. Energy Res.* 3 (2008) 204–214.
- [15] P. Sporn, E.R. Ambrose, The heat pump and solar energy, in: *Proceedings of the World Symposium on Applied Solar Energy* (1955). Phoenix, Ariz.
- [16] T.L. Freeman, J.W. Mitchell, T.E. Audit, Performance of combined solar-heat pump systems, *Sol. Energy* 22 (1979) 125–135.
- [17] A.R. Day, T.G. Karayiannis, Solar-assisted heat pump research and development, *Build. Serv. Eng. Res. T* 15 (1994) 71–80.
- [18] P.J. Martínez, A. Velázquez, A. Viedma, Performance analysis of a solar energy driven heating system, *Energy Buildings* 37 (2005) 1028–1034.
- [19] Z. Han, M. Zheng, F. Kong, F. Wang, Z. Li, T. Bai, Numerical simulation of solar assisted ground-source heat pump heating system with latent heat energy storage in severely cold area, *Appl. Therm. Eng.* 28 (2008) 1427–1436.
- [20] O. Ozgener, A. Hepbasli, Modeling and performance evaluation of ground source (geothermal) heat pump systems, *Energy Buildings* 39 (2007) 66–75.
- [21] Y.H. Kuang, R.Z. Wang, Performance of a multi-functional direct-expansion solar assisted heat pump system, *Sol. Energy* 80 (2006) 795–803.
- [22] G.Y. Xu, X.S. Zhang, S.M. Deng, A simulation study on the operating performance of a solar-air source heat pump water heater, *Appl. Therm. Eng.* 26 (2006) 1257–1265.
- [23] Y.W. Li, R.Z. Wang, J.Y. Wu, Y.X. Xu, Experimental performance analysis and optimization of a direct expansion solar-assisted heat pump water heater, *Energy* 32 (2007) 1361–1374.
- [24] F.X. Niu, L. Ni, M.L. Qu, Y. Yao, S.M. Deng, A study on a novel environmental control system with a triple sleeve energy storage exchanger, *Appl. Therm. Eng.* 54 (2013) 1–6.